AIP | Applied Physics Letters

Thermodynamics and kinetics of defects in Li2S

Ashkan Moradabadi and Payam Kaghazchi

Citation: Applied Physics Letters **108**, 213906 (2016); doi: 10.1063/1.4952434
View online: http://dx.doi.org/10.1063/1.4952434
View Table of Contents: http://scitation.aip.org/content/aip/journal/apl/108/21?ver=pdfcov
Published by the AIP Publishing

Thermodynamics and kinetics of defects in Li_2S

Ashkan Moradabadi[1,2] and Payam Kaghazchi[2,a)]
[1]*Institut für Materialwissenschaft, Fachgebiet Materialmodellierung, Technische Universität Darmstadt, Jovanka-Bontschits-Str. 2, 64287 Darmstadt, Germany*
[2]*Institut für Chemie und Biochemie, Freie Universität Berlin, Takustr. 3, 14195 Berlin, Germany*

(Received 2 December 2015; accepted 11 May 2016; published online 26 May 2016)

Li_2S is the final product of lithiation of sulfur cathodes in lithium-sulfur (Li-S) batteries. In this work, we study formation and diffusion of defects in Li_2S. It is found that for a wide range of voltages (referenced to metal Li) between 0.17 V and 2.01 V, positively charged interstitial Li (Li^+) is the most favorable defect type with a fixed formation energy of 1.02 eV. The formation energy of negatively charged Li vacancy (V_{Li}^-) is also constant, and it is only 0.13 eV higher than that of Li^+. For a narrow range of voltages between 0.00 V and 0.17 V, the formation energy of neutral S vacancy is the lowest and it decreases with decreasing the cell voltage. The energy barrier for Li^+ diffusion (0.45 eV), which takes place via an exchange mechanism, is 0.18 eV higher than that for V_{Li}^- (0.27 eV), which takes place via a single vacancy hopping. Considering formation energies and diffusion barriers, we find that ionic conductivity in Li_2S is due to both Li^+ and V_{Li}^-, but the latter mechanism being slightly more favorable. *Published by AIP Publishing.*
[http://dx.doi.org/10.1063/1.4952434]

Fundamental understanding of Li ion transport in solid electrode materials is of particular importance for the development of Li-based batteries (LiB) with high rate capabilities and high capacities. The process of Li^+ transport has thus been extensively studied in LiB anodes and cathodes using impedance spectroscopy and nuclear magnetic resonance as well as density functional theory (DFT) methods.[1–17] DFT calculations have provided detailed information on type of dominant ion carriers and their diffusion mechanisms in LiB.[14] It was found that Li diffusion occurs via Li vacancy in most cathode materials such as $LiCoO_2$ and $LiMnO_2$[15,18,19] as well as solid electrolyte materials such as $Li_7La_3Zr_2O_{12}$,[20] $Li_5La_3Ta_2O_{12}$,[20] and $Li_5La_3Nb_2O_{12}$,[21] while it takes place via interstitial Li in anode materials such as TiO_2.[22] Li transport via the exchange mechanism (–interstitial Li–Li site–interstitial Li–) has been reported in solid-electrolyte-interphase materials such as Li_2CO_3.[14] For large-scale applications such as grid-scale storages and electrical vehicles, lithium-sulfur (Li-S) batteries are more promising than LiB because of their high theoretical energy density (2600 W h/kg^{-1} (Ref. 23)), environmental friendly features, and low production cost.[24] During the discharge process, lithium ions react with the sulfur (S_8) cathode forming intermediate Li-polysulfides and finally crystalline Li_2S:[23,25–28] $S_8 \rightarrow Li_2S_8 \rightarrow Li_2S_6 \rightarrow Li_2S_4 \rightarrow Li_2S_2 \rightarrow Li_2S$. It is believed that diffusion of Li^+ in Li_2S is slow, and therefore, the formation of Li_2S crusts on the surface of sulfur cores during the lithiation process leads to an incomplete conversion of sulfur to Li_2S. Consequently, the measured discharge capacity is often less than the theoretical value.[25] Despite the importance of Li-S batteries, formation and diffusion of ions in Li_2S have not been studied so far. In this work, we calculated formation energies of possible defects and diffusion mechanism of the most favorable ones in Li_2S.

The DFT calculations were performed using the projector-augmented plane-wave code VASP.[29] Bulk Li_2S was modelled by $2\times2\times2$ super cells with $4\times4\times4$ Monkhorst-Pack k-point mesh with an energy cutoff of 360 eV. The diffusion pathways were calculated with the Nudge Elastic Band (NEB) method using 8 images. We have calculated the electronic and atomic structures as well as defect formation energies and diffusion barriers using the generalized gradient approximation (GGA) exchange-correlation functional proposed by Perdew, Burke, and Ernzerhof (PBE).[30]

In this work, we have considered the following types of defects: (1) neutral and charged Li vacancy (V_{Li} and V_{Li}^-), (2) neutral and charged interstitial Li (Li and Li^+), (3) neutral and charged S vacancy (V_S and V_S^{+2}), (4) neutral and charged interstitial S (S and S^{-2}), (5) neutral Li Frenkel (FR_{Li}), and (6) Li_2S Schottky (SC_{Li_2S}). Formation energies of defects were calculated by

$$\Delta E_d^{i,q} = E_{tot}^{i,q} - E_{tot}^{Li_2S} + \sum_i n_i\mu_i + q(\epsilon_F + \epsilon_{VBM}) + \Delta E, \quad (1)$$

where $E_{tot}^{i,q}$ and $E_{tot}^{Li_2S}$ are the total energies of defective and pristine Li_2S. n_i and μ_i are the number and chemical potential of defects (Li or S). We consider the dependence of the defect formation energy with respect to μ_{Li}, which is limited to a range within which Li_2S is thermodynamically stable with respect to bulk Li and S. Li crystal would start to form at the surface of Li_2S if μ_{Li} becomes too high (i.e., Li-rich limit). Moreover, since we are interested in $\Delta E_d^{i,q}$ as function of (half) cell voltage, we choose the zero value of μ_{Li} to be the chemical potential of Li-rich limit and define

$$\Delta\mu_{Li} = \mu_{Li} - \mu_{Li}^{rich} = \mu_{Li} - E_{Li}^{bulk}, \quad (2)$$

and obtain the (half) cell voltage with respect to Li electrode by

a)Electronic mail: payam.kaghazchi@fu-berlin.de

$$U = -\frac{\Delta\mu_{Li}}{e}, \tag{3}$$

where $E_{\mathrm{Li}}^{\mathrm{bulk}}$ is the total energy per atom of bulk Li with a bcc crystal structure (metal Li). Moreover, $\Delta\mu_{\mathrm{Li}}$ cannot be lower than a Li-poor limit below which Li_2S decomposes to sulfur. Therefore, in the defect formation energy plot, we also excluded the chemical potentials smaller than $\mu_{\mathrm{Li}}^{\mathrm{poor}} = \frac{1}{2}(\Delta G_{\mathrm{Li_2S}}^{\mathrm{bulk}})$ (half of the Gibbs free energy formation of bulk Li_2S). Our theoretical value of $\mu_{\mathrm{Li}}^{\mathrm{poor}} = 2.01\,\mathrm{eV}$ is 0.28 eV lower than the experimental value of $\mu_{\mathrm{Li}}^{\mathrm{poor}} = 2.29\,\mathrm{eV}$ ($\Delta G_{\mathrm{Li_2S}}^{\mathrm{bulk}} \approx -4.58\,\mathrm{eV}$ (Ref. 31)), which can be mainly because of using PBE functional and/or due to the fact that the theoretical value has been calculated at $T=0$ and $p=0$, while the experimental value has been measured at $T=298\,\mathrm{K}$ and $p=1\,\mathrm{bar}$. In this work, we assume that μ_{Li} can change freely between the Li-rich and Li-poor limits but μ_{S} has to satisfy this requirement

$$\mu_{\mathrm{S}} = E_{\mathrm{tot}}^{\mathrm{Li_2S}} - 2\mu_{\mathrm{Li}}, \tag{4}$$

where $E_{\mathrm{tot}}^{\mathrm{Li_2S}}$ is the total energy per formula unit of bulk Li_2S.

In Eq. (1), ϵ_F is the Fermi level (the energy of the electron reservoir in Li_2S), referenced to the bulk valence-band maximum (VBM) energy (ϵ_{VBM}). ΔE is the correction term to account for the finite-cell size effect of charged defects and also to align the electrostatic potentials of defective and pristine supercells. ΔE was calculated using the FNV approach[32,33] with the theoretical value of 3.6 for the dielectric constant.[34]

To calculate $\Delta E_{\mathrm{d}}^{i,q}$ and ϵ_{F} as function of $\Delta\mu_{Li}$, we assumed that all possible types of Li and S defects with concentrations of n_i as well as electrons and holes with concentrations of n_e and n_h, respectively, can exist simultaneously in Li_2S and applied the requirement of charge neutrality

$$\underbrace{\int_{\mathrm{CBM}}^{\infty} D(\epsilon) f(\epsilon,\epsilon_{\mathrm{F}})\,d\epsilon}_{n_{\mathrm{e}}} - \underbrace{\int_{-\infty}^{\mathrm{VBM}} D(\epsilon)\left[1 - f(\epsilon,\epsilon_{\mathrm{F}})\right] d\epsilon}_{n_{\mathrm{h}}}$$
$$= \sum_i q_i \underbrace{n_i^0 \exp\left(-\frac{\Delta E_{\mathrm{d}}^{i,q}}{k_B T}\right)}_{n_i}. \tag{5}$$

In this equation, $D(\epsilon)$ is the density of states, $f(\epsilon, \epsilon_{\mathrm{F}})$ is the Fermi-Dirac distribution $f(\epsilon,\epsilon_{\mathrm{F}}) = \{1 + \exp[(\epsilon - \epsilon_{\mathrm{F}})/k_{\mathrm{B}}T]\}^{-1}$, q_i is the charge state of defect i. n_{e}, n_{h}, and n_{i} are the concentration of electrons, holes, and defects of type i, while n_i^0 is the maximum possible concentration of defects of type i per unit volume. Since Eqs. (1) and (5) are self-consistent, $\Delta E_{\mathrm{d}}^{i,q}$ and ϵ_F were calculated iteratively.

Calculated defect formation energy and Fermi energy as function of $\Delta\mu_{Li}$ (Eq. (2)) and U (Eq. (3)) are illustrated in Figs. 1 and 2. It is found that for a wide range of $\Delta\mu_{Li}$ (U), namely, $-2.01\,\mathrm{eV} \le \Delta\mu \le -0.17\,\mathrm{eV}$ ($2.01\,\mathrm{V} \le U \le 0.17\,\mathrm{V}$), Li^{+1} is the most favorable defect type with a formation energy of 1.02 eV. At this range of Li chemical potential (cell voltage), V_{Li}^{-} is only 0.13 eV less favorable. The reason that the formation energy of charged defects in this range does not change with $\Delta\mu_{Li}$ (or U) is that increase in the Fermi energy and chemical potential of Li are equal and therefore cancel each other (see Eq. (1)). At the high chemical potential (low cell voltage) range of $-0.17\,\mathrm{eV} \le \Delta\mu_{Li} \le 0.00\,\mathrm{eV}$ ($0.17\,\mathrm{V} \le U \le 0.00\,\mathrm{V}$), V_S becomes the most favorable defect type. At this range, we find a decrease in the formation energy of Li^{+1} and increase in the formation energy of V_{Li}^{-}. This result is in line with a smaller increase of Fermi energy (see Fig. 2 and Eq. (1)) with $\Delta\mu_{Li}$ (decrease of U).

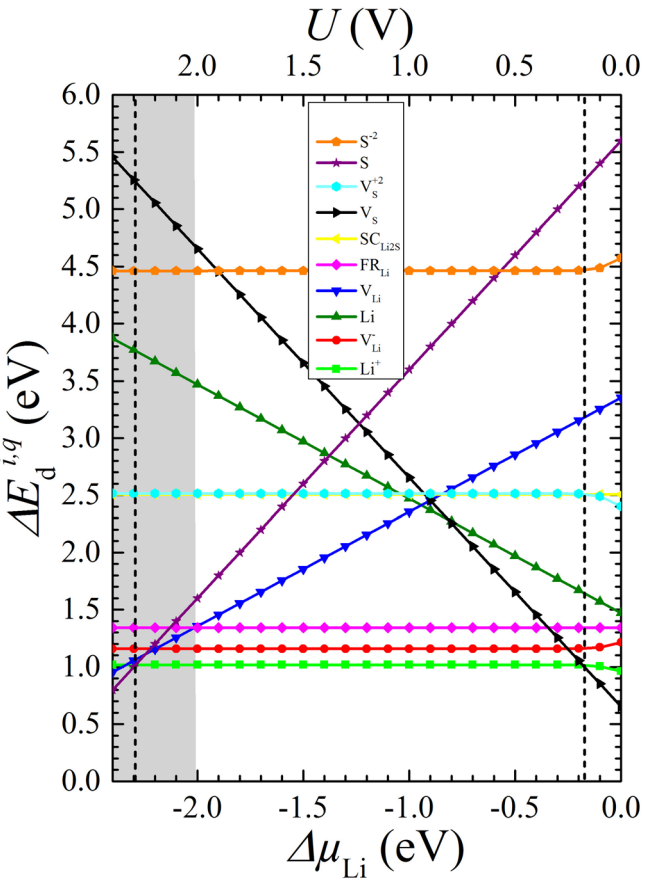

FIG. 1. Formation energies of different types of defects in bulk Li_2S as function of $\Delta\mu_{Li}$ and U. The chemical potential range of Li-poor limit is shaded in grey.

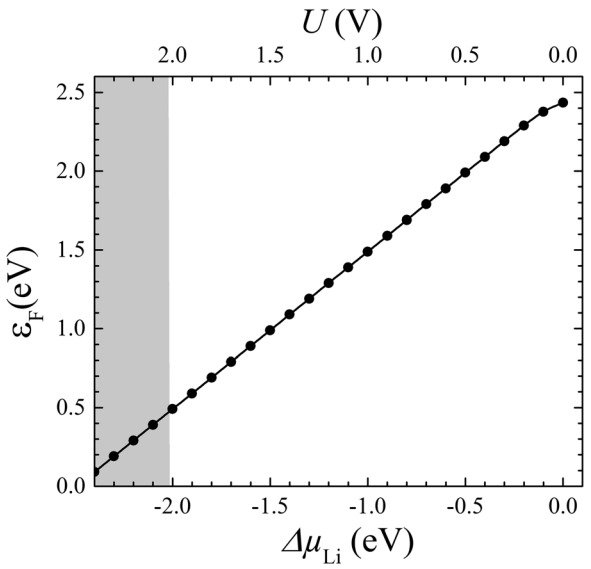

FIG. 2. Fermi energy of defective Li_2S as function of $\Delta\mu_{Li}$ and U. The chemical potential range of Li-poor limit is shaded in grey.

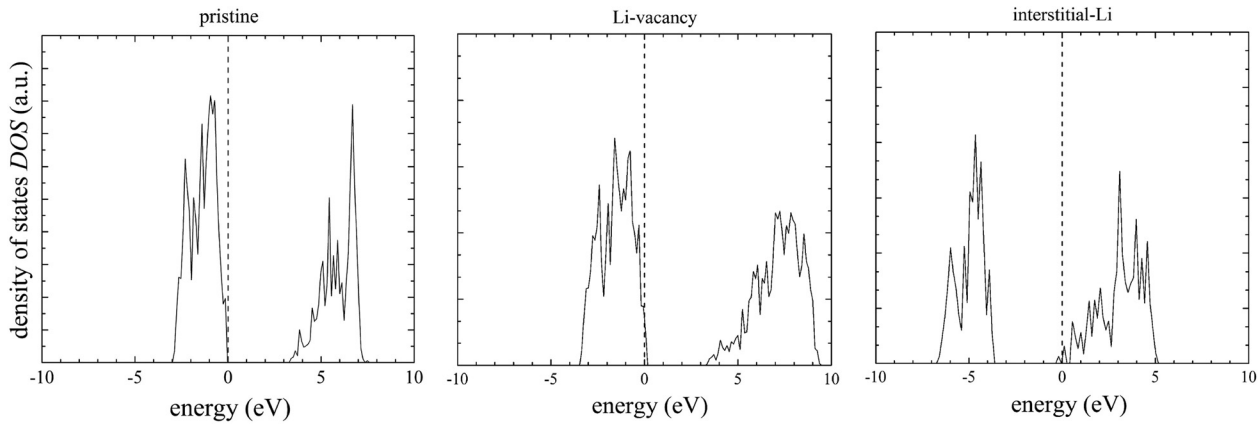

FIG. 3. Total density of states (DOS) of pristine, (Li) vacancy, and interstitial (Li) defective Li_2S calculated using GGA-PBE functional. The Fermi energy is set to zero.

The calculated total density of states for pristine as well as neutral vacant and interstitial Li is presented in Fig. 3. Bulk Li_2S is an indirect band gap semiconductor. The GGA-PBE band gap (E_g) calculated in this work is 3.24 eV, which is in agreement with the previous GGA-PBE values of E_g 3.36 eV (Ref. 34) and $E_g = 3.29$ eV.[35] It is known that GGA-PBE functional underestimates the width of band gap. We have not found any experimental measurement of E_g for Li_2S. To investigate the influence of underestimation of E_g on our results, defect formation energies were calculated for larger values of E_g (up to 4.00 eV). We found that the underestimation of E_g does not affect the conclusions of this work.

Afterwards, we studied Li diffusion for the following mechanisms:

(i) *Li hopping to nearby single and paired Li vacancy sites*. For the divacancy mechanism, we have considered orthogonal and diagonal move. Previous studies indicate that the diagonal pathway is the most favorable pathway for Li diffusion in most layered cathode materials in Li-ion batteries such as $LiCoO_2$ and $LiMnO_2$.[15,17] However, since S^{-2} ions are rather large in Li_2S, Li ions that move along the diagonal pathway fall to adjacent vacant sites. Therefore, the diagonal diffusion of Li to a divacancy in Li_2S is unlikely. The energy barrier (ΔE_b^{Li}) for orthogonal hopping of a Li to a divacant Li site ($\Delta E_b^{Li} = 0.20$ eV) is slightly lower than that to a single vacant site ($\Delta E_b^{Li} = 0.27$ eV). However, the total energy of a divacancy is 0.20 eV less favorable than two separated single vacancies. Therefore, Li hopping to a single vacancy is a more favorable mechanism than that to a divacant site (see Fig. 4 (left)).

(ii) *Li hopping between interstitial (octahedral) sites and also exchange of Li between interstitial sites and lattice sites*. We find that the exchange mechanism (see Fig. 4 (right)) has a diffusion barrier of $\Delta E_b^{Li} = 0.45$ eV, which is much lower than that of 1.58 eV for Li hopping between interstitial sites (which is not shown in Fig. 4).

Lithiation of a S cathode is known to start with the formation of Li_2S crusts on the outer surfaces of S particles and continue via a two-phase growth process,[36] during which nucleation and growth of Li_2S occurs at the Li_2S/S interface (see Fig. 5). Thus, the discharge capacity of S cathodes depends strongly on the activation energy barrier of Li ion transport within the Li_2S crusts, $\Delta E_a^{Li} = \Delta E_d^{Li} + \Delta E_b^{Li}$, which is the sum of formation energy and diffusion barrier. The calculated values of ΔE_a^{Li} in Li_2S are very high: 1.47 eV and 1.42 eV for Li^{+1} and V_{Li}^{-}, respectively.

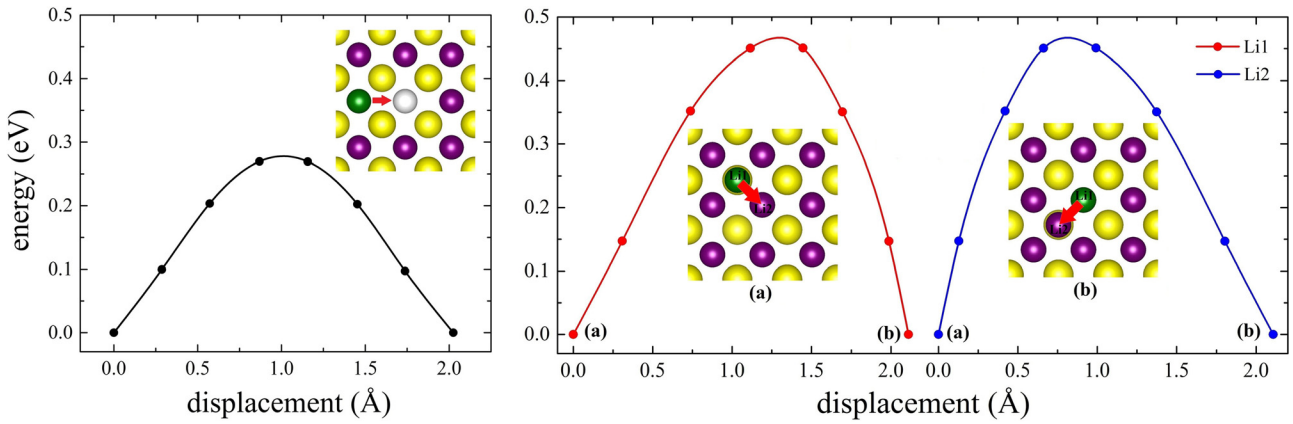

FIG. 4. Energy profiles and atomic structures for diffusion of (left) Li vacancy as well as (right) simultaneous diffusion of interstitial Li1 to Li2 site and Li2 site to the nearby empty interstitial site (exchange mechanism) in Li_2S. Li atoms are in violet, S atoms in yellow, diffusing Li atoms in green, and vacant sites in white.

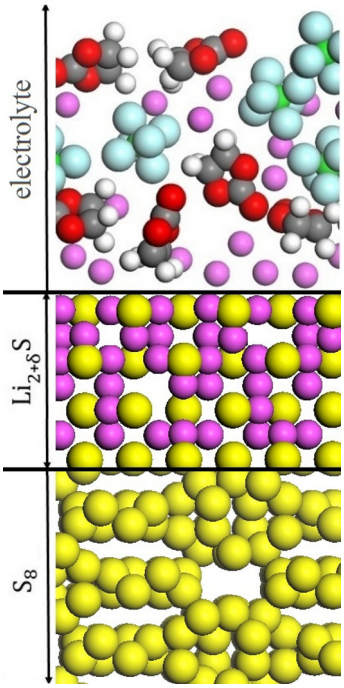

FIG. 5. Schematic of two-phase model for lithiation of sulfur (α-S_8) during the discharge process in Li-S batteries.

In summary, we have studied thermodynamics and kinetics of defects in Li_2S using *ab initio* calculations. According to the defect formation energy plot, positively charged interstitial Li is 0.13 eV more favorable than negatively charged Li vacancy almost for the whole range of cell voltages relevant to Li-S battery, where charge and discharge take place, namely $1.5\,V \leq U \leq 2.4\,V$.[37,38] However, the diffusion barrier is 0.18 eV lower in the latter case. We found that the activation energy for formation and diffusion of negatively charged Li vacancy is 0.05 eV lower than the positively charged interstitial Li, which may show a more dominant role of the former defect type in Li ion conductivity of Li_2S. Calculated activation energies for Li transport in Li_2S are very high, explaining why the measured discharge capacity is lower than the theoretical value.

The authors gratefully acknowledge support from the "Bundesministerium für Bildung und Forschung" (BMBF), the computing time granted on the Hessian high performance computer "LICHTENBERG" at Technische Universität Darmstadt and Zentraleinrichtung für Datenverarbeitung (ZEDAT) at the Freie Universität Berlin.

[1]H. Buschmann, J. Dölle, S. Berendts, A. Kuhn, P. Bottke, M. Wilkening, P. Heitjans, A. Senyshyn, H. Ehrenberg, A. Lotnyk, V. Duppel, L. Kienle, and J. Janek, "Structure and dynamics of the fast lithium ion conductor $Li_7La_3Zr_2O_{12}$," Phys. Chem. Chem. Phys. **13**(43), 19378–19392 (2011).
[2]A. Kuhn, S. Narayanan, L. Spencer, G. Goward, V. Thangadurai, and M. Wilkening, "Li self-diffusion in garnet-type $Li_7La_3Zr_2O_{12}$ as probed directly by diffusion-induced 7Li spin-lattice relaxation NMR spectroscopy," Phys. Rev. B **83**, 094302 (2011).
[3]L. V. Wüllen, T. Echelmeyer, H. W. Meyer, and D. Wilmer, "The mechanism of Li-ion transport in the garnet $Li_5La_3Nb_2O_{12}$," Phys. Chem. Chem. Phys. **9**, 3298–3303 (2007).
[4]S. P. Ong, V. L. Chevrier, G. Hautier, A. Jain, C. Moore, S. Kim, X. Ma, and G. Ceder, "Voltage, stability and diffusion barrier differences between sodium-ion and lithium-ion intercalation materials," Energy Environ. Sci. **4**(9), 3680–3688 (2011).
[5]H. Xia, L. Lu, and G. Ceder, "Li diffusion in $LiCoO_2$ thin films prepared by pulsed laser deposition," J. Power Sources **159**, 1422–1427 (2006).
[6]D. Morgan, A. Van der Ven, and G. Ceder, "Li conductivity in Li_xMPO_4 (M = Mn, Fe, Co, Ni) olivine materials," Electrochem. Solid State Lett. **7**(2), A30–A32 (2004).
[7]A. Van der Ven, G. Ceder, M. Asta, and P. D. Tepesch, "First-principles theory of ionic diffusion with nondilute carriers," Phys. Rev. B **64**(18), 184307-1–184307-17 (2001).
[8]A. Van der Ven and G. Ceder, "Lithium diffusion mechanisms in layered intercalation compounds," J. Power Sources **97–98**, 529–531 (2001).
[9]P. Kaghazchi, "Phase-sensitivity of Li intercalation into Sn," J. Phys.: Condens. Matter **25**(38), 382204 (2013).
[10]P. Kaghazchi, "Mechanism of Li intercalation into Si," Appl. Phys. Lett. **102**, 093901 (2013).
[11]E. Lee and K. A. Persson, "Li absorption and intercalation in single layer graphene and few layer graphene by first principles," Nano Lett. **12**(9), 4624–4628 (2012).
[12]A. Dunst, V. Epp, I. Hanzu, S. A. Freunberger, and M. Wilkening, "Short-range Li diffusion vs. long-range ionic conduction in nanocrystalline lithium peroxide Li_2O_2 the discharge product in lithium-air batteries," Energy Environ. Sci. **7**, 2739–2752 (2014).
[13]O. Gerbig, R. Merkle, and J. Maier, "Electron and ion transport in Li_2O_2," Adv. Mater. **25**, 3129–3133 (2013).
[14]S. Shi, P. Lu, Z. Liu, Y. Qi, L. G. Hector, H. Li, and S. J. Harris, "Direct calculation of Li-ion transport in the solid electrolyte interphase," J. Am. Chem. Soc. **134**, 15476–15487 (2012).
[15]A. Moradabadi and P. Kaghazchi, "Mechanism of Li intercalation/deintercalation into/from the surface of $LiCoO_2$," Phys. Chem. Chem. Phys. **17**, 22917 (2015).
[16]J. Rohrer, A. Moradabadi, K. Albe, and P. Kaghazchi, "On the origin of anisotropic lithiation of silicon," J. Power Sources **293**, 221–227 (2015).
[17]T. Zhang, D. Li, Z. Tao, and J. Chen, "Understanding electrode materials of rechargeable lithium batteries via DFT calculations," Prog. Nat. Sci. **23**(3), 256–272 (2013).
[18]A. Van der Ven and G. Ceder, "Lithium diffusion in layered Li_xCoO_2," Electrochem. Solid-State Lett. **3**, 301 (2000).
[19]D. Kramer and G. Ceder, "Tailoring the morphology of $LiCoO_2$: A first principles study," Chem. Mater. **21**, 3799 (2009).
[20]L. J. Miara, S. P. Ong, Y. Mo, W. D. Richards, Y. Park, J. M. Lee, H. S. Lee, and G. Ceder, "Effect of Rb and Ta doping on the ionic conductivity and stability of the garnet $Li_{7+2x-y}(La_{3-x}Rb_x)(Zr_{2-y}Ta_y)O_{12}$ ($0 \leq x \leq 0.375$, $0 \leq y \leq 1$) superionic conductor: A first principles investigation," Chem. Mater. **25**, 3048–3055 (2013).
[21]X. Yu, W. Xian-Ping, G. Yun-Xia, H. Jing, Z. Zhong, G. Li-Jun, F. Qian-Feng, and L. Chang-Song, "Correlation of lithium ionic diffusion with Nb concentration in $Li_{7-x}La_3Zr_{2-x}Nb_xO_{12}$ evaluated by an internal friction method," Chin. Phys. Lett. **31**(1), 016201 (2014).
[22]M. Wagemaker, *Structure and Dynamics of Lithium in Anatase TiO_2* (Delft University Press, 2003).
[23]L. Chen and L. L. Shaw, "Recent advances in lithium-sulfur batteries," J. Power Sources **267**, 770–783 (2014).
[24]L. Wang, Y. Wang, and Y. Xia, "A high performance lithium-ion sulfur battery based on a Li_2S cathode using a dual-phase electrolyte," Energy Environ. Sci. **8**, 1551 (2015).
[25]Y. Yang, G. Zheng, and Y. Cui, "Nanostructured sulfur cathodes," Chem. Soc. Rev. **42**, 3018 (2013).
[26]K. Kumaresan, Y. Mikhaylik, and R. E. White, "A mathematical model for a lithium-sulfur cell," J. Electrochem. Soc. **155**, A576 (2008).
[27]B. Scrosati, J. Hassoun, and Y. K. Sun, "Lithium-ion batteries. A look into the future," Energy Environ. Sci. **4**, 3287 (2011).
[28]P. G. Bruce, S. A. Freunberger, L. J. Hardwick, and J. M. Tarascon, "Li-O_2 and Li-S batteries with high energy storage," Nat. Mater. **11**, 19 (2012).
[29]G. Kresse and J. Furthmüller, "Efficient iterative schemes for *ab initio* total-energy calculations using a plane-wave basis set," Phys. Rev. B **54**, 11169 (1996).
[30]J. P. Perdew, K. Burke, and M. Ernzerhof, "Generalized gradient approximation made simple," Phys. Rev. Lett. **77**, 3865 (1996).
[31]D. R. Lide, *CRC Handbook of Chemistry and Physics*, 87th ed. (CRC Press, 2006).
[32]C. Freysoldt, J. Neugebauer, and C. G. Van de Walle, "Fully *ab initio* finite-size corrections for charged-defect supercell calculations," Phys. Rev. Lett. **102**, 016402 (2009).

[33]C. Freysoldt, J. Neugebauer, and C. G. Van de Walle, "Electrostatic interactions between charged defects in supercells," Phys. Status Solidi B **248**, 1067–1076 (2011).
[34]H. Khachai, R. Khenata, A. Bouhemadou, A. Haddou, A. H. Reshak, B. Amrani, D. Rached, and B. Soudini, "FP-APW+lo calculations of the electronic and optical properties of alkali metal sulfides under pressure," J. Phys.: Condens. Matter **21**, 095404 (2009).
[35]R. D. Eithiraj, G. Jaiganesh, G. Kalpana, and M. Rajagopalan, "First-principles study of electronic structure and ground-state properties of alkali-metal sulfides - Li_2S, Na_2S, K_2S and Rb_2S," Phys. Status Solidi B **244**, 1337–1346 (2007).
[36]R. Xu, I. Belharouak, X. Zhang, R. Chamoun, C. Yu, Y. Ren, A. Nie, R. Shahbazian-Yassar, J. Lu, J. C. M. Li, and K. Amine, "Insight into sulfur reactions in Li-S batteries," ACS Appl. Mater. Interfaces **6**, 21938–21945 (2014).
[37]D. Bresser, S. Passerini, and B. Scrosati, "Recent progress and remaining challenges in sulfur-based lithium secondary batteries – a review," Chem. Commun. **49**, 10545–10562 (2013).
[38]G. L. Xu, Q. Wang, J. C. Fang, Y. F. Xu, J. T. Li, L. Huanga, and S. G. Sun, "Tuning the structure and property of nanostructured cathode materials of lithium ion and lithium sulfur batteries," J. Mater. Chem. A **2**, 19941–19962 (2014).